doi: 10.1111/j.1751-3928.2007.00014.x *Resource Geology* Vol. 57, No. 2: 149–169

Original Article

Gold-Related Sulfide Mineralization and Ore Genesis of the Penjom Gold Deposit, Pahang, Malaysia

Kamar Shah Ariffin[1] and Nick J. Hewson[2]

[1]*School of Materials and Mineral Resources Engineering, Universiti Sains Malaysia, Nibong Tebal, Penang and*
[2]*Specific Resources, Kuala Lipis, Pahang, Malaysia*

Abstract

The Penjom gold deposit lies on the eastern side of the Raub-Bentong Suture line within the Central Belt of Permo-Triassic rocks, near Kuala Lipis, Pahang, Malaysia. The geology of the deposit is dominated by a sequence of fine- to coarse-grained rhyolitic to rhyodacitic tuff, tuff-breccia and a minor rhyolitic–rhyodacitic volcanic series, associated with argillaceous marine sedimentary rocks consisting of shale with subordinate shalely limestone of Padang Tungku Formation and Pahang Volcanic Series. Fine- to coarse-grained tonalite and quartz porphyry intruded this unit. The main structural features of the area are north–south-trending left-lateral strike-slip faults and their subsidiaries, which generally strike north–south and dip moderately to the east (350°–360°/40°–60°). Mineralization at the Penjom gold deposit is structurally controlled and also erratic laterally and vertically. The gold mineralization can be categorized as (i) gold associated with carbonate-rich zones hosted within dilated quartz veins carrying significant amount of sulfides; (ii) gold disseminated within stockwork of quartz–carbonate veins affiliated with tonalite; and (iii) gold often associated with arsenopyrite and pyrite in quartz–carbonate veins and stringers hosted within shear zones of brittle–ductile nature in all rock types and in brittle fractured rhyodacitic volcanic rocks. Sphalerite, chalcopyrite, tetrahedrite and pyrrhotite are the minerals accompanying the early stage of gold mineralization. These minerals also suffered from local brittle deformation. However, most of the gold mineralization took place after the deposition of these sulfides. Galena appears somewhat towards the end of gold mineralization, whereas tellurium and bismuth accompanied gold contemporaneously. The gold mineralization occurred most probably due to the metamorphogenic deformational origin concentrated mostly in the shear zone. The mineralization is strongly controlled by the wall rock (e.g. graphitic shale), the sulfide minerals and fluid–rock interaction.

Keywords: alteration minerals, gold mineralization pattern, metallogeny, ore genesis, orogenic gold deposit, ore microscopy, paragenesis.

1. Introduction

Malaysia is a highly prospective region for gold and it has a long history of widespread small-scale gold mining throughout the country, especially in the Central Belt of Peninsula Malaysia. Long before the development of the great gold-fields such as in South Africa, Australia and USSR, Malaysia had already established itself as one of the important gold producer (Santokh Singh, 1977; Becher, 1983; Chu & Singh, 1984). Prior to the Portuguese conquest of Malacca in 1511, the country was known as the "Aurea Chesonese" or "Golden Peninsula". The majority of the gold production apparently came from the states of Pahang and Kelantan within the Central Belt (Fig. 1). A study of literatures covering the geology of the Central Belt goldfield

Received: 3 August 2006. Accepted for publication 28 January 2007.
Corresponding author: K. S. ARIFFIN, School of Materials and Mineral Resources Engineering, Universiti Sains Malaysia, Nibong Tebal, Penang, 14300 Malaysia. Email: kamarsha@eng.usm.my

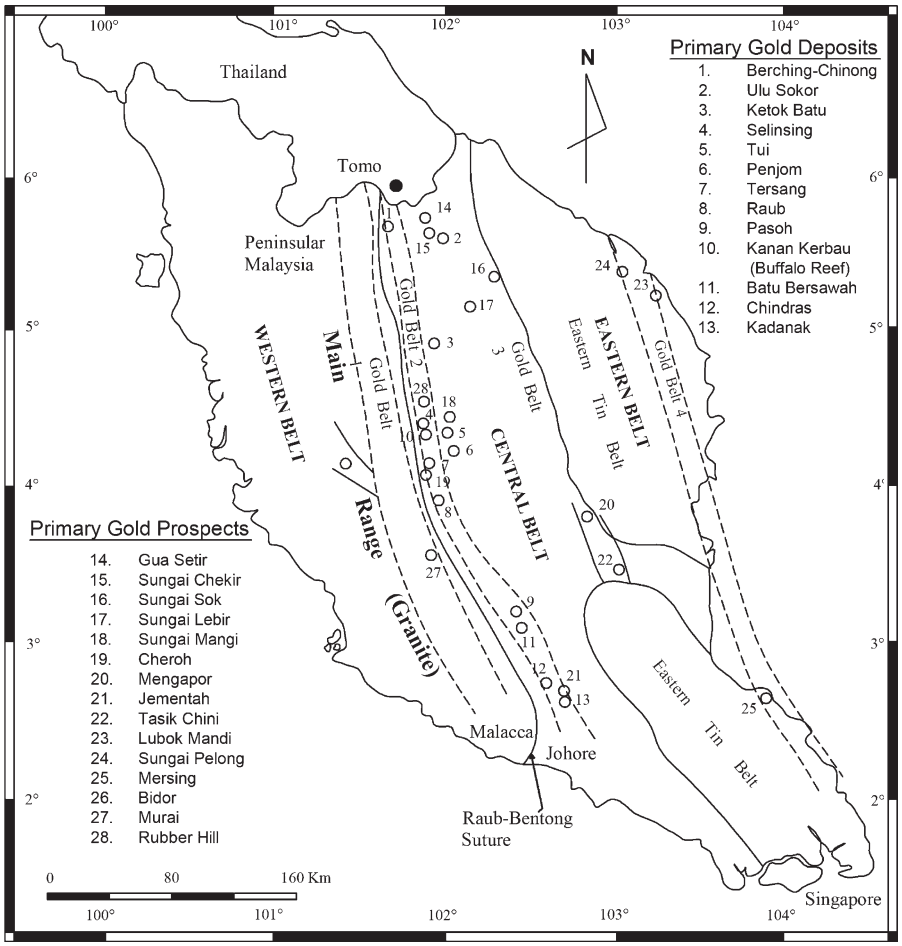

Fig. 1 Peninsula Malaysia showing mineral belts and primary gold occurrences (modified after Yeap, 1993).

shows the important role of hydrothermal fluids in the formation of gold deposits (Scrivenor, 1911, 1928, 1931; Richardson, 1939, 1950; Alexander, 1949; Proctor, 1972; Lee *et al.*, 1982, 1986; Yeap, 1993). The regional geochemical survey for gold, carried out by Mineral and Geosciences Department of Malaysia over the Central Belt in North Pahang and South Kelantan, has defined a 20-km-wide, north–south-trending gold mineralization in the Raub-Kuala Medang-Lipis-Merapoh area (Fig. 2). Several mines being worked extensively were alluvial deposits developed on vein stockworks in altered, brecciated and sheared intrusive or adjacent country rocks. Attraction lies on the good possibilities of the existence of sizeable tonnage of low-grade gold deposit.

Major primary gold mineralization patterns within Central Belt can be grouped into two types: type I (gold belt 2) and type II (gold belt 3), respectively. The type I deposits consist of significantly large quartz reefs/lodes and parallel swarms of vein, traversing metasediments and granite. This type I mineralization belt is also identified as the gold geochemical zone (Lee *et al.*, 1982, 1986). The mineralization is confined within brittle–ductile shear or brecciated zones. This gold belt is located immediately to the east of the Main Range granite and Raub–Bentong line (Yeap, 1993). Two major goldfields within the type I belt are the Buffalo reef (Kanan Kerbau) and further south, the Selinsing gold mine and the Tersang alluvial goldfields. Enhanced level and occurrences of stibnite and scheelite are common characteristics of the Buffalo reef, Selinsing and Raub goldfields, whereas ilmenite and cassiterite occurrence is considerable at the Tersang goldfield (Pereira, 1993; Pereira *et al.*, 1993; Kamar Shah & Khairun Azizi, 1995). However, elevated As and Sb are considered a common trend of these goldfields. Type II, which is located immediately to the east of the type I deposits, exhibits a broader variety of gold mineralization, bounded to gold disseminated within a stockwork

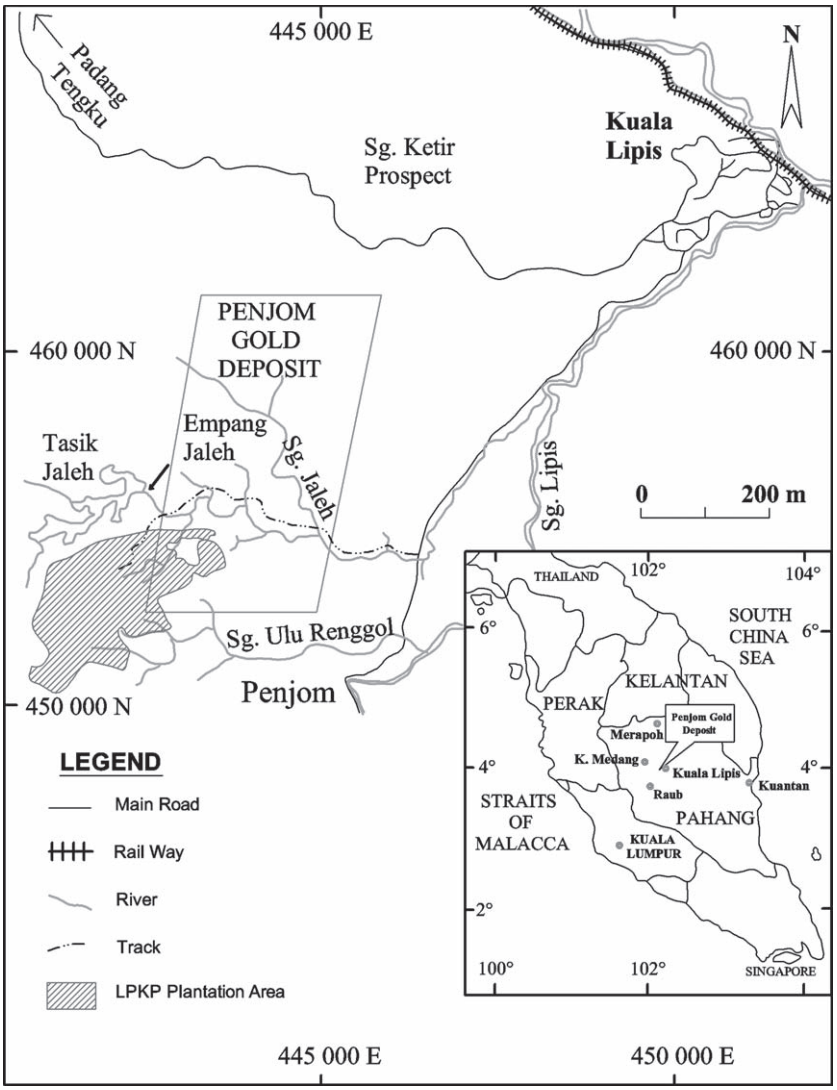

Fig. 2 Location of the Penjom gold deposit.

of quartz veins affiliated with intrusive bodies and volcanogenic exhalative sulfides within a shear zone system. Dilated quartz veins and Au-Ag-bearing skarn carry significant amount of sulfides (Sinjeng, 1993). The type II belt is also designated as the silver zone (Lee *et al.*, 1986). Gold belt 4 (Lubok Mandi-Mersing Belt) is located in the eastern part of Peninsula Malaysia and it is juxtaposed with the Eastern Tin Belt. The Lubok Mandi gold deposit is an 8-km gold–quartz lode hosted in weakly metamorphosed and folded slate, phyllite and meta-arenites. In the Mersing area the primary gold mineralization was observed as several discontinuous, approximately 350° striking, gold–quartz veins cutting strongly folded meta-argillites and arenites (Yeap, 1993).

The Penjom gold deposit is one of the promising goldfields currently being mined within the eastern side of the Bentong Suture line of the type II gold mineralization pattern of the Central Gold belt, which is located near Kuala Lipis, Pahang (Fig. 2) as a low-grade and bulk-mineable deposit. The Penjom gold deposit is distinctly associated with Tertiary, volcanic and hydrothermal activity broadly related to plate boundaries in the Asian region. However, geologically mesothermal deposits are more important in Peninsula Malaysia compared to epithermal gold, as suggested by the findings of Corbett (2002).

Investigation was achieved through comprehensive soil geochemistry data (Fig. 3) and materials (Tables 1–3) compiled from 3234 m of east–west-trending exploration

trenches, diamond drill cores with total length of 1399.45 m (25 holes) and grab samples collected during the early stage of an exploration program conducted to evaluate and delineate the extent of gold mineralization over the prospect. The drill holes have advanced to an average depth of 100 m and were drilled within a mineralized section at an angle between 40° and 60°.

Mineralized and unmineralized sections including alteration materials and specimens from 25 diamond drill holes acquired from this exploration program were analyzed. Specimens of the core sample were prepared for petrography and ore microscopy (Jenalab model, Carl Zeiss polarizing microscope, Carl Zeiss, Germany), Vicker's microhardness (VHN; 6758, Leitz Wetzlar, Germany), X-ray diffraction (XRD; PW 1820, Philips, UK), scanning electron microscope (SEM; Stereoscan 200 Cambridge Instruments, Cambridge, UK), inductively coupled plasma (ICP; Optima 3000XL, Perkin Elmer, Malaysia), energy-dispersive X-ray spectroscopy (EDX) microprobe (Stereoscan 200, equipped with AN 10000 software system, Cambridge Instruments), AAS (1100B model, Perkin Elmer), fluid inclusion (USGS-type gas-flow heating/freezing stage, Natural Heritage Museum, London) and X-ray fluorescence (XRF; RIX 3000, Rigaku, Japan) analyses. The mode of occurrences and distribution, mineralogical, geochemical and textural characteristics of gold and other sulfide mineralization at the Penjom gold deposit was examined. The relationship between lithogechemistry of the unmineralized and mineralized zones with mineralogical and distribution trends associated with gold mineralization was established to facilitate ore genesis.

2. Geology and mineralization

2.1. Regional tectonic setting

Peninsula Malaysia is a part of the east Eurasian Plate and tectonically located to the north of currently active subduction zones of the Sunda arc. Gold discovery in this region is always associated with Tertiary volcanic and hydrothermal activities, and appears to be very broadly related to tectonic boundaries.

The Malay Peninsula may be divided into two tectono-stratigraphic terranes that form part of the Eurasian Terrane, namely the East Malay (Eurasian plate-Indochina) terrane and the Sibumasu (Shan-Thai) terrane, respectively. The Eurasian Terrane (Manabor block) has been interpreted as a Permo-Triassic island arc system that has never been separated very far from the Shan-Thai block (Fig. 4). Stratigraphic,

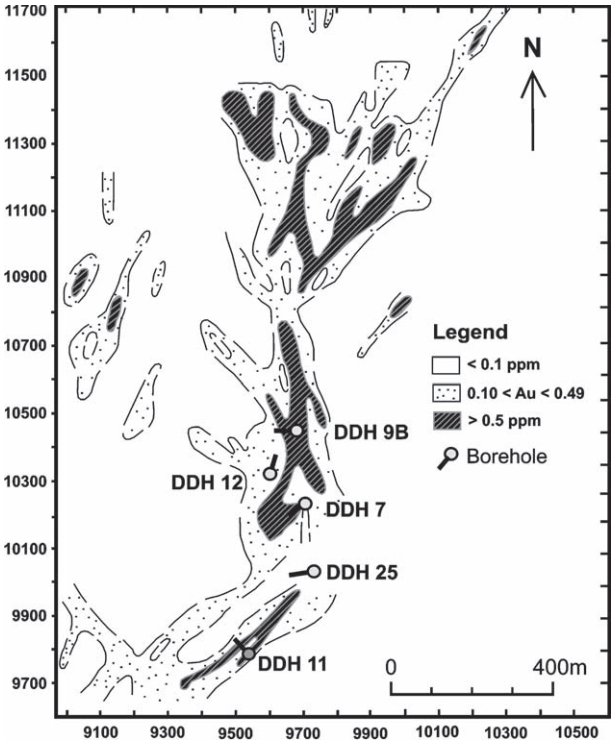

Fig. 3 Generalized soil geochemistry anomaly of the Penjom gold deposit.

paleontological and palaeomagnetic evidence suggests that a possible origin of these terranes was rifting of the north-east margin of the ancient Gondwana landmass in the Late Permian–Early Triassic, which was responsible for the formation of the Central Belt and the Raub-Bentong Suture (Kobayashi & Toriyama, 1970; Mitchell, 1977; Khoo & Tan, 1983; Tan, 1984, 1996; Tjia, 1987, 1989; Metcalfe, 1988, 2000, 2002; Yeap, 1993; Schwartz *et al.*, 1995; Spiller & Metcalfe, 1995; Campi *et al.*, 2002; Cocks *et al.*, 2005). Thus a thin and irregular strip of continental lithosphere and island arc sequence developed in front of it. These detachments later collided with the accreting Asian landmass and fused along the Raub-Bentong Suture. Peninsula Malaysia to the east of the suture belongs to Cathaysia. A collision structure overprint has generated major N-S- or NW-SW-trending left-lateral strike-slip fault and dilational Riedal and subsidiary shears associated with these fault (Tjia & Zaitun, 1985; J. N. Hewson & D. A. Crips, unpubl. data, 1992).

The Raub-Bentong Suture is a deep rooted 13 km-wide tectonic zone that runs generally in the N-S direction from Tomo in Thailand (Fig. 1) along the east side margin of the Main Range to the Malacca-Johore border

Table 1 Chemical composition of various rock materials, mineralized and unmineralized sections

	DDH-9B	DDH-25	DDH-7	DDH-12	DDH-12	DDH-25
DDH >	(1)	(2)	(3)	(4)	(5)	(6)
SiO_2 (%)	64.23	42.53	70.82	75.92	42.79	62.27
TiO_2	0.57	0.05	0.05	0.12	0.05	0.57
Al_2O_3	16.90	2.70	15.45	7.82	16.93	16.49
Fe_2O_3	6.38	8.04	1.25	3.24	13.59	7.03
MnO	0.21	0.27	0.05	0.05	0.12	0.07
MgO	<0.01	4.18	<0.01	<0.01	<0.01	2.33
CaO	0.26	20.27	1.69	2.69	6.57	1.63
Na_2O	<0.01	<0.01	5.65	<0.01	1.46	3.02
K_2O	3.38	<0.01	1.14	1.52	1.76	1.78
P_2O_5	0.07	<0.01	<0.01	0.06	<0.01	0.07
L.O.I	5.59	21.02	2.62	2.97	8.94	4.30
As (ppm)	98	5589	33	1518	430	44
Cr	61	357	267	79	26	78
La	29	28	29	28	30	29
Sr	50	206	108	72	91	99
W	<5	5	<5	5	<5	<5
Y	27	23	27	<5	24	27
Sn	<30	<30	<30	<30	<30	<30
Ta	<3	<3	3	3	3	<3
Nb	27	23	34	26	34	26
Pb	45	63	40	212	84	39
Cu	<5	<5	<5	<	<5	8
Zn	452	182	38	44	1606	81
S	<20	11464	1811	9844	40193	1069

1, grey tuff (27.50 m); 2, graphitic shale (32.80 m); 3, tonalite (62.90 m); 4, yellowish-grey gold-bearing tonalite (77.73 m): fault gouge materials; 5, black grey felsite (tonalite) (84.00 m): fault gouge materials; 6, grey tuff (119.00 m).

(Tan, 1984, 1996; Metcalfe, 1988, 1992, 2000, 2002; Tjia, 1989; Yeap, 1993; Cocks *et al.*, 2005). This N-S zone is located some 20 km to the west of the Penjom gold deposit. This zone is characterized by the presence of schist, cherts with small serpentine bodies, argillite, olistostrome and mélange (Tjia, 1987; Metcalfe, 2000). It is also a zone of parallel steeply dipping N-S faults with several periods of reactivation. The Gold belt lies in the East Malay/Indochina Block (Fig. 4), subdivided into Eastern Belt and Central Belt (Fig. 1). The Penjom gold deposit lies within the western margin of the Central Belt (gold belt 3).

The Central Belt consists mainly of Permo-Triassic, low-grade metasediments, deep to shallow marine clastic sediments and limestone with abundant intermediate to acid volcanics and volcaniclastics, deposited in a paleo-arc basin (Richardson, 1939; Proctor, 1972; Gobbett & Hutchison, 1973; Leman, 1994; Metcalfe, 2002). Batholiths in the Eastern Belt are smaller than those of Sibumasu, but are, in comparison, compositionally expanded. The Jurassic–Late Cretaceous batholiths, dominantly monzogranitic suite are of I-type affinity and carry both precious and base metals. Magmatism in the Central Belt is markedly less common and consists of an alkali series ranging from gabbro-diorite (157 Ma), monzonite (163 Ma) to quartz syenite (127 Ma), and a later calc-alkali series of granodiorites and granites (Bignell & Snelling, 1977; Hutchison, 1977; Ahmad, 1979; Khoo & Tan, 1983; Mohd Rozi & Sheikh Almashoor, 2000; Yong *et al.*, 2004). The Central Belt granitoids, which lie critically close to the Raub-Bentong Suture line, have large ion lithophile elements, that is, Ba and Sr, nearly 1000 times rock/mantles and classified as mantle plume-type magmatism (Mustaffa Kamal & Azman, 2003; Azman *et al.*, 2006). The Benom Plutonic Complex (Early Jurassic) which comprises Bukit Lima, is the nearest shoshonitic granitoid to the Penjom in the south (Figs 5, 6), characterized by high K_2O content.

Mineralization in the Central Belt is dominated by gold. The old Raub gold mine lies within the western side of the Central Belt, whereas the Mengapur copper–gold porphyry skarn prospect is situated on the northeastern side (Fig. 1). Both deposits carry significant gold mineralization. Widespread alluvial gold occurrences have been long recognized in this area and there

Table 2 Geochemical data of various grab samples from Penjom

Site no	Local easting	Local northing	Field description	Au	Ni	Co	Ag	Mo	Cu	Pb	Zn	Fe	Mn	As	Sn	W	Hg	Sb	Bi	Ba	Cr	Se	Te
10	9510	9770	Shale,carb	5.55	3	1	3.8	4.7	184	146	6	3.2	9	42,704	10	12	0.06	36	20	30	1		
10a	9490	9760	Qv	2.45	4	2	0.8	4.7	22	44	6	1.5	12	18,168	5	12	0.02	10	5	27	1		
10b	9500	9770	Tuff, bleached	83.37	1	1	20.0	4.1	67	64	6	4.2	9	63,963	5	16	0.02	22	7	76	1		
10c	9760	10,580	Felsite silic	0.01	3	1	0.2	3.9	6	250	11	0.1	13	200	5	4	0.02	2	8	22	1		
39	9720	10,120	Porphyry	0.08	1	1	0.2	3.8	3	62	7	0.2	29	80	5	28	0.02	6	10	43	25		
1170	9620	9870	F.breccia	19.46	9	1	0.6	2.2	12	161	6	0.4	330	564	5	80	0.06	2	11	65	24	0.1	0.1
1503	9560	10,410	Shale	0.01	8	2	0.1	2.4	35	19	14	1.9	202	100	5	2	0.02	1	2	50	12		
1504	9550	10,410	Qv	0.02	9	2	0.1	1.9	31	13	31	4.5	1636	300	5	2	0.02	1	1	36	14		
1507	9593	10,090	Qv	10.98	7	1	0.3	2.9	52	58	8	1.6	367	2018	5	20	0.04	1	2	34	7	0.1	0.7
1508	9650	9905	Qv	0.22	6	1	1.9	2.1	28	40	6	0.9	785	1855	5	20	0.02	1	1	54	10	0.1	0.5
1509	9630	9670	Shale	0.01	14	15	0.1	2.6	23	16	26	1.3	153	40	10	4	0.02	1	1	37	8		
1513	9960	9540	Qv	0.01	1	3	0.3	2.5	39	36	108	23.0	257	100	10	2	0.04	1	1	29	16		
1514	9610	10,980	Qv	0.07	8	1	0.3	1.9	7	45	8	0.6	693	150	10	36	0.02	2	2	36	7		
1516	9840	11,040	Qv	1.67	40	17	1.8	183.0	128	760	440	22.0	7600	9273	10	4200	0.12	1	6	105	9	0.1	0.9
1517	9841	11,040	Qv	1.84	5	1	0.4	4.9	7	35	6	1.1	585	5273	5	20	0.02	5	1	119	5	0.5	0.5
1518	9840	11,050	Qv	26.13	2	1	1.3	17.5	26	540	9	8.5	136	107,363	10	20	0.12	130	19	320	9	0.5	7.7
1519	9470	11,860	Qv	0.13	8	1	0.2	3.1	31	24	21	2.2	1020	600	5	2	0.02	1	1	43	11	0.1	0.2
1521	9040	9690	Qv	0.87	14	5	20.0	2.8	103	370	30	2.9	1252	5091	5	8	0.04	7	9	89	15	0.5	0.5
1522	9000	9750	Iron oxide	0.04	20	43	4.6	3.2	59	960	260	26.0	18,680	200	5	12	0.10	1	3	194	28		
1523	9250	10,110	Tuff, silic	0.01	2	2	0.2	2.7	7	17	12	0.8	132	20	5	2	0.02	1	1	40	2		
1525	10,420	12,240	Tuff	0.01	4	2	0.2	2.2	10	58	6	0.5	586	30	5	4	0.02	1	5	44	4		
1528	10,395	12,160	Qv	0.15	5	2	0.4	2.9	20	250	11	1.3	1012	100	5	20	0.02	1	8	62	10		
1530	9740	15,080	Shale calc	0.01	5	1	0.1	9.4	23	13	31	0.5	1111	10	10	2	0.02	5	3	669	5		
1531	10,410	12,185	Shale, silic	0.00	9	20	0.2	2.3	85	8	98	10.1	1357	20	5	2	0.02	1	1	85	11		
1532	9340	9670	Porphyry	0.02	2	1	0.1	2.3	2	173	3	0.3	282	200	5	2	0.02	1	2	51	4		
1533	9700	10,105	Porphyry	0.02	2	1	0.1	2.6	4	430	2	0.2	155	140	5	28	0.02	1	9	42	3		
1534	10,410	12,183	Shale, silic	0.00	2	1	0.1	2.1	6	12	3	0.6	108	5	5	2	0.02	1	1	46	3		
1535	9635	10,300	Tuff, silic	0.00	0	0	0.0	0.0	0	0	0	0.0	0	0	0	0	0.00	0	0	0	0		

All elements in ppm, except Fe%; Pt, Pd, Rh, ppb.

Table 3 Geochemical data for borehole DDH-11and DDH-12 samples

Site No.	Field description	BH No	Top Depth (m)	Bottom Depth (m)	Au	Ni	Co	Ag	Mo	Cu	Pb	Zn	Fe	Mn	As	Sn	W	Hg	Sb	Bi	Ba	Cr	Se	Te	Pt	Pd	Rh
3175	Shale+ qv + py/aspy	11	14.00	16.00	1.98	30	22	0.8	1.1	17	61	39	5.7	1747	17273	20	4	0.02	14	1	23	44	0.5	4.3	1	1	1
3176	Shale/tuff, py + aspy,	11	16.00	18.00	0.45	18	14	0.6	2.8	16	12	37	4.2	1102	5546	5	4	0.06	3	1	25	12					
3177	Tuff/shale, py + aspy,	11	18.00	20.00	0.20	15	13	0.6	2.7	47	28	53	3.5	620	3818	5	2	0.02	1	1	40	19					
1154	Tuff with coarse aspy	11	18.80	19.80	1.91	19	17	1.9	1.6	50	93	47	3.7	522	8909	5	12	0.02	1	4	31	30	0.1	1.2	1	1	1
3178	Tuff/shale, py + aspy,	11	20.00	22.55	0.75	16	17	0.9	3.2	44	16	27	3.2	418	8909	5	2	0.02	1	3	31	19	0.5	0.5			
3179	Felsite	11	22.55	25.00	0.05	2	1	1.9	4.1	3	31	5	0.6	181	1818	5	2	0.02	1	10	49	48					
3180	Felsite + f. gouge	11	25.00	27.50	0.53	4	3	1.4	4.5	3	34	11	0.8	250	3364	5	2	0.02	1	7	26	51					
1155	Felsite, porphyritic	11	27.20	28.00	0.02	1	1	1.2	1.1	50	31	8	0.3	139	200	5	2	0.02	1	3	24	15					
3181	Felsite/qv+ sulphides	11	27.50	30.85	0.49	62	10	1.7	4.4	10	34	18	1.2	476	1818	5	4	0.02	1	11	105	100					
1200	Felsite	11	28.20	29.00	0.03	4	1	2.2	1.6	11	49	7	0.4	221	909	5	2	0.02	1	12	45	66	0.1	1.0			
1157	Tuff, with abundant, aspy,	11	30.85	31.15	18.54	29	18	4.0	2.5	81	109	19	5.9	246	85000	10	20	0.02	48	11	24	33	0.5	8.6	1	1	1
3182	F.gouge, qv+ abundant sulphide	11	30.85	31.40	47.33	28	14	8.1	6.4	40	78	10	6.5	642	82364	5	4	0.02	44	7	37	44	0.5	8.3	4	1	1
3183	Felsite + f. gouge	11	31.40	33.00	3.77	15	7	1.5	6.2	5	25	9	3.1	808	28909	5	2	0.02	11	4	154	59					
1156	Felsite, banded	11	31.70	32.00	0.09	2	1	0.7	1.1	3	20	5	0.7	368	3455	10	2	0.02	1	1	28	13					
1158	Qv, sulphide-rich	11	32.40	32.65	12.32	38	22	3.7	9.2	7	36	8	5.9	512	69818	10	12	0.02	50	6	68	100	0.5	7.6	5	2	1
3184	F. breccia + sulphide	11	33.00	34.60	1.52	10	6	1.2	6.6	10	27	15	3.4	1001	9364	5	2	0.02	1	5	145	24					
3185	Tuff	11	34.60	36.30	0.10	13	12	0.9	3.1	11	22	10	2.1	493	60	5	2	0.02	1	3	75	11					
3186	Shale, fractured + py/aspy	11	36.30	38.90	0.08	17	8	0.2	4.4	13	12	15	2.6	1502	2909	30	2	0.04	1	1	253	25					
1159	Shale, graphitic shale	11	36.50	37.40	0.12	11	6	1.0	7.2	12	18	14	2.7	628	150	5	2	0.02	1	1	48	18	1.3	0.5			
3187	Tuff/lst	11	38.90	41.00	0.02	11	7	0.3	2.7	9	9	13	1.6	1390	30	5	2	0.04	1	1	132	22					

continued

Table 3 Continued

Site No.	Field description	BH No	Top Depth (m)	Bottom Depth (m)	Au	Ni	Co	Ag	Mo	Cu	Pb	Zn	Fe	Mn	As	Sn	W	Hg	Sb	Bi	Ba	Cr	Se	Te	Pt	Pd	Rh
1160	Tuff, fine with calc- bands	11	40.30	40.80	0.00	4	3	0.7	4.4	6	10	13	1.1	2005	30	5	4	0.02	1	2	368	12					
3188	Shale	11	41.00	43.40	0.00	9	5	0.1	4.2	12	16	16	1.8	2166	25	5	4	0.04	3	1	128	17					
3189	Tuff	11	43.40	45.50	0.00	17	13	0.3	2.0	19	14	22	3.1	1757	400	5	4	0.04	2	1	102	22					
3190	Tuff	11	45.50	47.90	0.01	15	12	0.1	2.1	20	12	15	2.5	892	25	5	4	0.02	1	2	68	24					
3191	Lst/calc shale, py	11	47.90	51.00	0.02	16	10	0.3	4.0	20	14	22	2.1	1430	545	5	4	0.04	2	2	175	17					
1161	Lst, shelly, abundant py	11	50.60	50.80	0.02	13	9	0.7	4.9	16	14	18	2.1	932	35	5	2	0.02	1	2	225	13	1.4	0.3			
3192	Shale	11	51.00	53.00	0.02	10	3	0.3	6.7	11	8	19	1.1	3240	25	20	4	0.02	1	3	296	10					
3193	Shale, local fracturing	11	53.00	55.00	0.03	13	10	0.2	4.2	26	4	22	2.5	1377	2182	5	4	0.02	1	2	81	20					
3194	Shale, local fracturing	11	55.00	57.60	0.02	17	15	0.1	1.4	34	1	18	3.3	579	1455	5	4	0.02	1	1	46	16					
1163	Shale with qv	11	55.30	55.60	0.01	13	14	0.6	2.4	40	1	17	2.8	641	200	5	4	0.02	1	1	47	9	0.2	0.4			
3195	Tuff, calc	11	57.60	60.00	0.01	12	9	0.4	2.6	14	15	17	2.1	1249	364	5	4	0.04	2	1	92	23					
3196	Tuff, calc	11	60.00	63.55	0.00	11	7	0.2	3.6	15	8	29	1.9	1489	15	5	4	0.06	2	6	57	27					
1164	Tuff	11	62.50	63.10	0.00	11	10	0.8	1.6	20	12	37	2.0	432	15	5	4	0.02	1	1	25	41					
3197	Lst/shale	11	63.55	66.50	0.01	14	11	0.1	3.9	21	11	65	2.6	1141	1091	5	4	0.06	4	1	109	22					
1165	Shale and lst, banded	11	65.00	65.60	0.00	9	3	0.5	7.8	9	12	34	0.9	4930	15	5	2	0.02	1	1	150	7					
3198	Lst/shale	11	66.50	69.30	0.02	14	9	0.2	4.9	21	10	58	1.7	1275	909	5	4	0.04	1	5	488	21					
1166	Shelly lst	11	68.80	69.30	0.01	6	3	0.4	7.6	9	13	25	0.8	3930	35	5	4	0.02	1	1	569	6					
3205	Felsite, weathered, qv	12	12.00	14.00	0.63	4	1	1.5	1.9	69	49	8	0.3	104	909	5	4	0.02	1	11	31	10					
3206	Felsite, weathered, qv	12	14.00	16.00	0.19	4	1	1.8	1.2	7	19	5	0.2	166	818	5	4	0.02	5	10	28	9					
3207	Felsite, weathered, qv+py/aspy	12	16.00	18.00	1.71	8	2	5.4	5.0	168	145	19	1.3	356	4091	5	20	0.02	4	5	30	10					
1192	Qv, rare	12	17.20	17.80	0.07	7	1	0.5	2.7	19	23	9	0.4	12	2727	5	2	0.02	2	1	43	220	0.1	0.7	1	1	1
1192A	Qv, iron stained	12	17.20	17.80	7.77	7	2	6.8	65.0	171	640	62	4.4	49	2763	5	140	0.02	6	4	39	150	0.1	7.2	1	1	1
3208	Felsite+vuggy qv+py/aspy	12	21.60	24.50	3.74	8	1	5.3	2.6	87	66	17	1.0	293	1000	5	28	0.02	1	7	35	25	0.1	1.1	3	1	1
3209	Felsite	12	24.50	27.00	0.04	5	1	0.1	1.8	26	10	23	0.6	47	382	5	12	0.02	1	1	29	6	0.1	0.4			
3210	Felsite	12	27.00	30.00	0.01	9	4	0.3	1.1	22	8	34	1.0	279	364	5	12	0.02	1	1	31	11					
1193	Felsite	12	29.70	30.90	0.03	5	3	0.2	1.0	7	8	40	1.2	41	200	5	8	0.02	1	1	37	8	0.1	0.1			
3211	Felsite	12	30.00	34.00	0.04	7	2	0.2	2.5	13	2	28	1.1	57	527	5	8	0.02	1	1	29	57					
3212	Felsite	12	34.00	38.00	0.05	8	6	0.2	1.0	30	7	38	2.5	1699	909	5	2	0.02	1	1	29	7					

continued

Table 3 Continued

Site No.	Field description	BH No	Top Depth (m)	Bottom Depth (m)	Au	Ni	Co	Ag	Mo	Cu	Pb	Zn	Fe	Mn	As	Sn	W	Hg	Sb	Bi	Ba	Cr	Se	Te	Pt	Pd	Rh
3213	Fine banded felsic tuff	12	38.00	42.00	0.10	5	5	0.3	1.1	5	2	31	2.1	1517	545	5	2	0.02	1	1	33	6					
1194	Tuff, fine, banded	12	42.00	43.50	0.00	2	2	0.2	0.6	6	5	22	1.2	708	200	5	2	0.02	1	1	45	17					
3214	Fine banded felsic tuff	12	42.00	46.00	0.05	3	4	0.1	1.1	12	5	26	1.7	1270	909	5	2	0.02	1	1	43	9					
3215	Fine banded felsic tuff	12	46.00	50.00	0.03	5	5	0.2	1.0	15	9	25	1.4	1278	891	5	2	0.02	1	1	41	9					
3216	Felsite+qv, with py, aspy, gal	12	50.00	52.00	0.05	6	1	3.5	1.2	10	209	18	0.5	572	1273	10	4	0.02	1	11	30	51					
3217	Felsite + qv, with py, aspy, gal	12	52.00	54.00	0.18	7	1	5.3	1.4	9	300	24	1.2	301	8636	10	4	0.02	1	20	33	63					
3218	Felsite + qv, with py, aspy, gal	12	54.00	57.60	0.02	7	1	1.1	1.0	14	82	12	0.4	830	364	20	8	0.02	1	2	46	28					
3219	Felsite + qv, with py, aspy, gal	12	57.60	60.00	0.07	3	3	0.3	2.2	19	29	14	0.6	1536	273	5	4	0.02	2	2	130	21					
3220	Felsite + qv, with py, aspy, gal	12	60.00	62.00	0.00	4	1	0.7	2.6	28	48	77	0.6	1678	1000	5	2	0.02	2	1	58	41					
3221	Felsite + qv, sulphide rich	12	62.00	64.00	3.89	4	17	104.0	7.3	460	7000	630	7.1	825	30182	5	2	0.02	10	270	122	61	0.5	19.5	1	1	1
3222	Felsite + qv, sulphide rich	12	64.00	66.00	0.75	2	2	20.0	11.1	57	2070	59	1.2	4660	1273	5	2	0.02	1	41	562	33					
3223	Felsite + qv, sulphide rich	12	66.00	68.00	0.34	1	2	1.8	5.2	43	156	60	1.7	390	3982	5	2	0.02	1	4	52	47					
3224	Felsite + qv, sulphide rich	12	68.00	70.00	0.44	1	2	2.9	4.3	157	350	45	2.7	277	4182	5	2	0.02	1	5	67	57					
3225	Felsite, little qv	12	70.00	73.00	0.04	4	2	0.5	2.3	31	56	27	1.1	655	545	5	12	0.02	1	1	77	23					
1198	Felsite	12	71.70	72.20	0.02	1	2	0.2	1.0	28	17	45	0.9	297	400	5	4	0.02	1	1	64	30					
3226	Felsite, little qv	12	73.00	75.00	0.14	2	3	0.2	2.3	16	13	64	1.3	989	20	5	8	0.02	3	1	138	18					
1197	Q-carb v, visible Au	12	81.00	82.00	148.00	4	4	67.0	3.4	1420	2800	1460	7.9	2920	1382	5	2	0.14	8	25	547	260	0.5	17.5	1	2	1
3233	Felsite	12	87.50	90.00	0.34	3	1	2.9	1.3	10	153	15	0.3	672	364	5	4	0.02	1	11	51	30					
3234	Felsite	12	90.00	93.10	0.02	5	1	1.5	2.4	20	62	9	0.5	828	545	5	2	0.02	1	11	55	33					

All elements in ppm except Fe%; Pt, Pd, Rh, ppb.

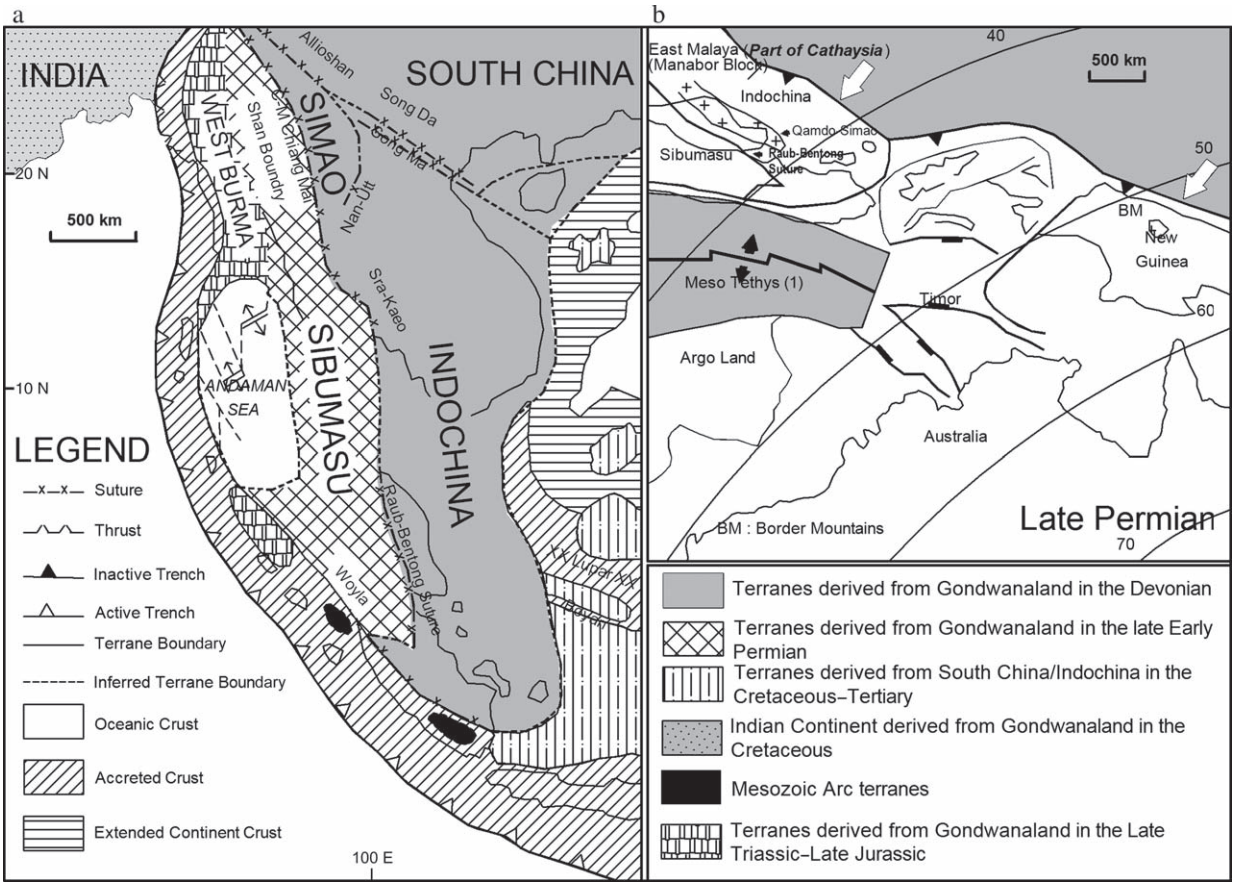

Fig. 4 (a) Distribution of continental blocks, fragments, terranes and principal sutures of Southeast Asia, and (b) palaeogeography during the Late Permian to show the position of Sibumasu, East Malaya/Indochina and Raub-Bentong Suture (modified after Metcalfe, 2002).

is a total in excess of 1 million ounces (28,400 kg) of gold recovered. Therefore, the Central Belt is well-known as the Gold Belt (Scrivenor, 1911). Acid and intermediate intrusive rocks were emplaced east and parallel to Raub-Bentong Suture.

2.2. Geological setting of Penjom area

Geology of the Penjom gold deposit is dominated by the widespread occurrences of marine clastic sediments, intermediate to acid volcaniclastics, and subordinate rhyolitic lava sequences (Fig. 7). These volcaniclastics are predominantly of tuff, with occasional lava and agglomerate, tuff breccia that are mostly rhyolitic to rhyodacitic in composition. These rocks are interbedded mainly with carbonaceous shale and less frequently with limestone and confined to Permian and Lower Triassic. The bulk of Permian belongs to so-called Padang Tengku Formation, a Raub Group rock assemblage and Pahang Volcanic Series (Fig. 6). Underlying this unit in the western flank is the older Sungai Sergis Formation, which is composed of a thick sequence of shale with very minor limestone intercalation and much thicker bands of tuff containing fragments of both rhyolite and andesite (Scrivenor, 1928, 1931; Richardson, 1939; Alexander, 1949; Nancy, 1972; Proctor, 1972; Gobbett & Hutchison, 1973; Nuraiteng, 1993; Leman, 1994; Kamar Shah, 1995; Campi *et al.*, 2002).

Rhyodacitic tuff of varying color, from grey and greenish-grey to buff pinkish brown, is the major rock type in the mineralized zone. They are composed mainly of solidified ash and coarse-grained clast-supported tuff breccias or agglomerate. This rock unit is often interbedded or intercalated with shale and siltstone, less frequently, with dark black limestone in

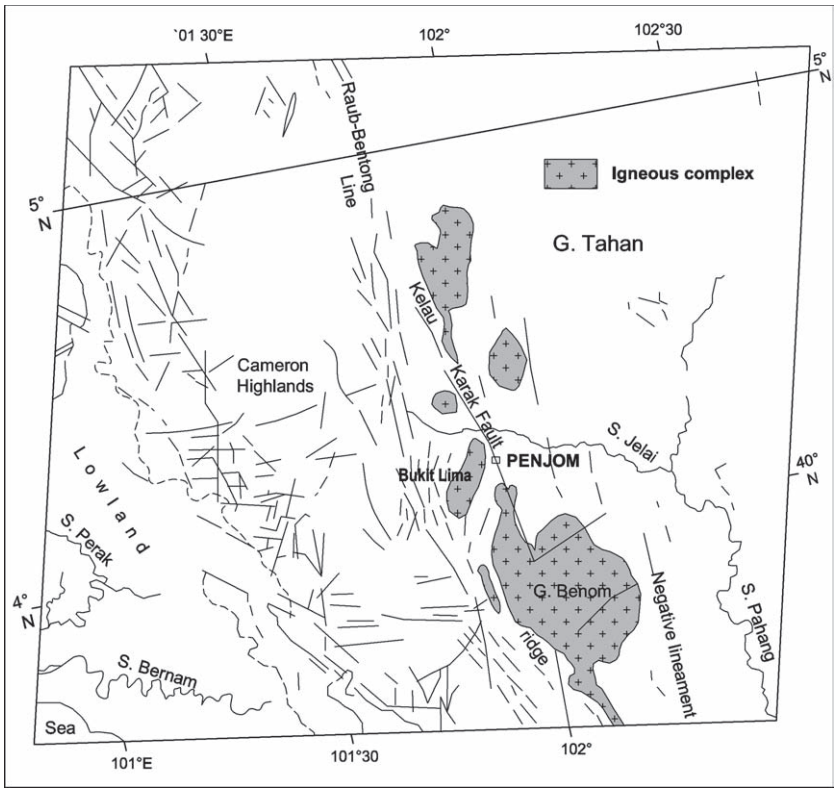

Fig. 5 Geometrical pattern of district-scale fault trends and numerous splays running along the Central Gold Belt with major granitoid emplacement (after Tjia & Zaitun, 1985).

places. The shale is often carbonaceous and dark in color with disseminated pyrite cubes in places.

This volcaniclastic and sedimentary association is intruded by a few shallow dipping sheets of tonalite as narrow sills and minor dykes of quartz porphyries that run sub-parallel to the main mineralized shear zone (Penjom thrust). Tonalite is a major igneous intrusion in the area. This homogeneous, fine- to medium-grained, white or buff to pinkish brown and highly competent tonalite is generally composed of >54% plagioclase, 7% orthoclase, and >30% quartz (Kamar Shah, 1995). This unit is often found interfingered and folded along other rocks, and appeared soft and friable (sugary fell) when highly decomposed into *in situ*, light grey sandy clay. The tonalite of the area intruded with minimal thermal aureoles at 400°C between 5 and 10 km depth (I. Bogie, unpubl. data, 2002; Flindell, 2003).

2.3. Structural setting and mineralization

The Raub-Bentong Suture has accommodated considerable strike–slip movement. Structural analysis indicated a regular geometrical pattern of district-scale fault trends that can be observed within most goldfields in the Central Belt. The Kelau–Karak fault is one of the major faults running across the Penjom gold field, as indicated by Tjia and Zaitun (1985) in relation to the structure elements that control major plutonic emplacements (Fig. 5). This has resulted in numerous splays running along the Central Gold Belt. The Penjom gold deposit is located along one of the significant splays. In general, the stratigraphic sequence of sedimentary rocks at Penjom strike N–S and dips moderately to the east, which coincides with the regional N-S strike and with emplacement of granitoid bodies. Localized disruption is caused by faulting and folding, and within the deposit the Penjom thrust has an EW strike and southerly dip.

Mineralization at the Penjom gold deposit is structurally controlled and erratic laterally and vertically. The Penjom thrust is the dominant feature controlling the distribution of ore at Penjom and generally strikes NE (35°) and dips to the southeast (30–40°). Considerable shear movements along the Penjom thrust have remobilized much of the carbon within the shale sequence to form a graphitic alteration zone. This, together with

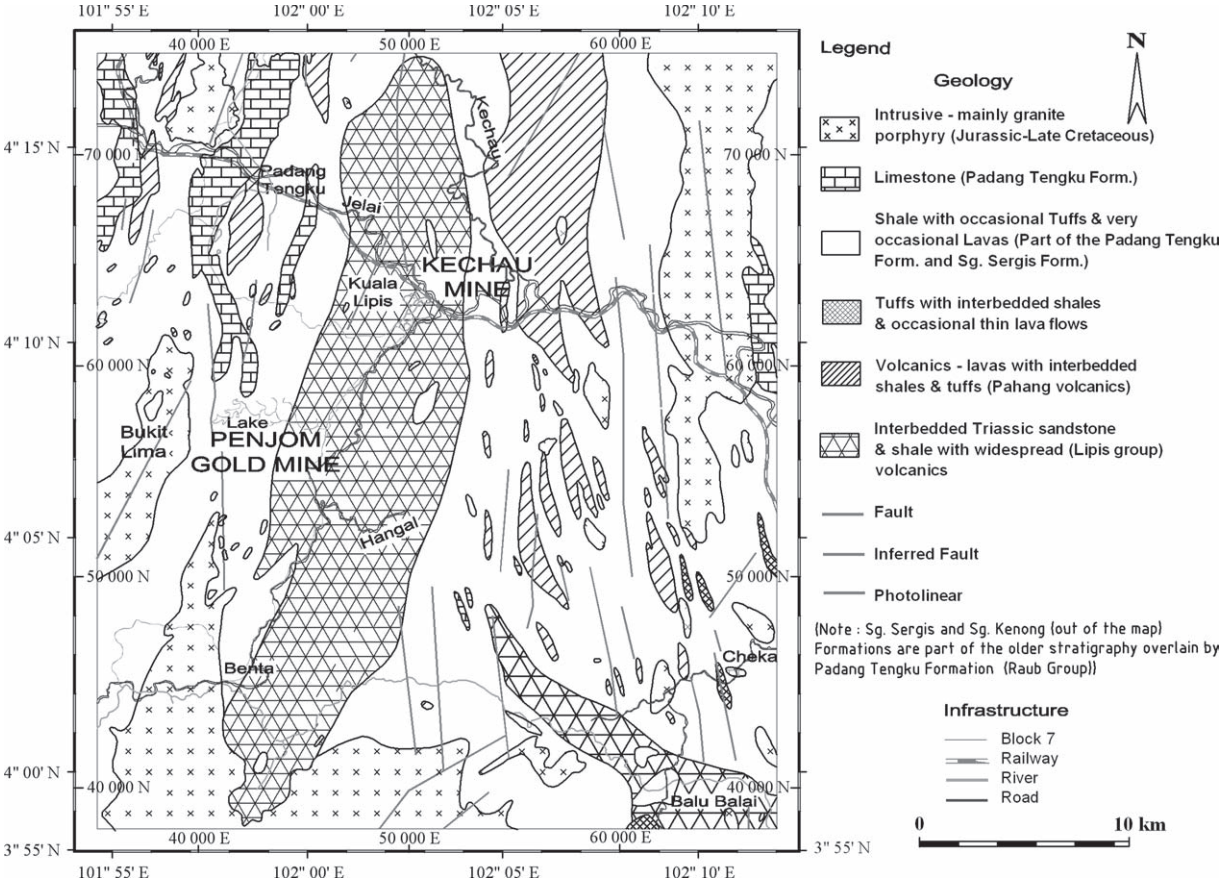

Fig. 6 Geology of the Benta-Lipis area (after Alexander, 1949; Proctor, 1972; J. N. Hewson & D. A. Crips, unpubl. data, 1992).

sheared and milled rock (fault gouge materials), makes the Penjom thrust an impermeable zone (J. N. Hewson & D. A. Crips, unpubl. data, 1992; Kamar Shah, 1995; R. Kidd, unpubl. data, 1998; Sonny *et al.*, 2001). Major gold mineralization took place within the footwall of this thrust (Fig. 8).

The mineralization can be categorized into (i) gold associated with carbonate-rich zones hosted within dilated quartz veins carrying significant amount of sulfides; (ii) gold disseminated within stockwork of quartz–carbonate veins affiliated with tonalite; and (iii) gold that is associated with arsenopyrite and pyrite in quartz carbonate veins and stringers hosted within shear zones of brittle–ductile nature in all rock types and in brittle fracture in rhyodacitic volcanics. The mineralized zone is normally located within the shallow zone not exceeding 100 m.

Major gold mineralization is observed along the steeply dipping faults. However, there is no significant gold mineralization above the Penjom thrust (Fig. 8), with only discrete late-stage quartz–carbonate-galena veins and later calcite veins and stringers in hanging wall (Kamar Shah, 1995; Fillis, 2000; Sonny *et al.*, 2001; Flindell, 2003). Gold mineralization is related to discontinuous, strike-restricted (metre-scale) quartz–ankerite–dolomite–sulfide veins. Kamar Shah (1995), Kamar Shah and Khairun Azizi (1995), Fillis (2000) and Sonny *et al.* (2001) described the types and sites of quartz–carbonate veins including (i) ribbon veins along bedding planes; (ii) lamellae-banded veins along and adjacent to NS- and NW-striking faults (particularly within the Penjom thrust); and (iii) fracture-hosted veins becoming stockwork in and on the contact of tonalite intrusions.

Favorable settings for high-grade veins are the contact between tonalite and carbonaceous sedimentary rocks, especially where the latter are carbonaceous and/or the strata are tightly folded or intensely faulted.

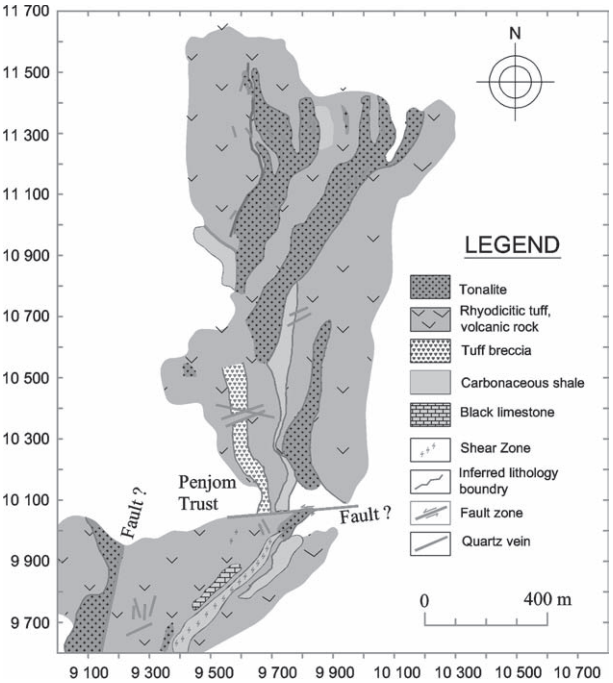

Fig. 7 Geology of the Penjom gold deposit.

Fillis (2000) highlighted fold hinges as particularly well-mineralized sites. Competency contrasts and the chemical activity of carbon are primary factors in focusing gold mineralization (Kamar Shah, 1995; Sonny *et al.*, 2001).

2.4. Alteration characteristics

Hydrothermal alteration accompanying gold mineralization at Penjom is weak and localized. Wall rock alteration at Penjom is due to the interaction or association with hydrothermal activity, igneous intrusion, quartz veining and faulting. Three dominant types of alteration recognized are silicification, argillic alteration and chloritization, marked by a prolific development of secondary minerals over the primary mineral (Kamar Shah, 1995; Wan Fuad & Heru Sigit, 2001). The bleaching and narrow silicified zones are notable. Limonitic iron staining is widespread. Phyllic and propylitic alteration are widespread with sericite (illite)–quartz–chlorite–albite. Carbonate minerals are associated with tonalite intrusion and sedimentary rock adjacent to dacitic and rhyodacitic rocks. Pervasive silicification is often found as quartz veining close to shear zones. Sericitization occurs within the rhyolite, tuffaceous sediments and tonalites. Chloritization occurs in the furthermost zone outside the silicification and argillic zones, characterized by the presence of chlorite, epidote and carbonate. This chloritization of ferromagnesian minerals, pyritization and carbonization are also present within tuffaceous and shale units. K/Ar dating of sericite separates yielded ages of 194–191 Ma (I. Bogie, unpubl. data, 2002).

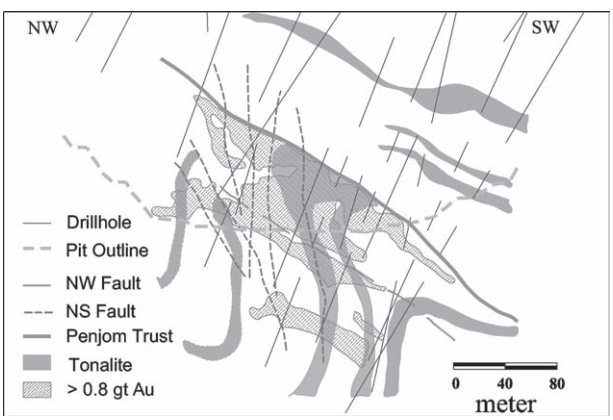

Fig. 8 Cross-section across the Penjom ore body running through the centre of the main deposit (after Flindell, 2003).

3. Lithogeochemistry

Chemical composition of selected materials that represent rocks from grab samples and boreholes DDH 11 and DDH 12 (Figs 3, 9) are presented in Tables 1 and 2. Sulfide minerals such as arsenopyrite, pyrite, chalcopyrite, sphalerite and galena are prominent in many samples associated with gold mineralization. Sulfides seem abundant in zones associated with fault gouge materials that host much of the gold mineralization at Penjom, within carbonaceous or graphitic shale and brecciated tuff in proximity or within felsic intrusive rock, especially within the footwall. This zone is also characterized by heavily fractured quartz veins. Gold-bearing quartz-carbonate veins and stockwork are intercepted in various rock types.

Multi-elemental distribution patterns with respect to the depth, geochemistry and structural features of the Penjom gold deposit as from DDH11 (Fig. 10) and DDH-12 show that most of the gold-rich samples are proportionally elevated in arsenic. Silver, As, Te, Sb, and Bi except Hg from DDH-11 and DDH-12 are most elevated in the segments associated with sulfide-gold mineralization. Gold has a marked affinity with Te and Bi and less with Sb. Two of the mineralized samples hosted within tuff of DDH-11, which are characterized by fault gouge materials have shown compelling

occurrence of As (80,000 ppm), Au (18–47 ppm), Ag (4–8 ppm) and Te (8.5 ppm).

Other signatures conspicuously associated with gold are Ba, Mo, Co, Ni, W and Se. These elements in most cases show a more sporadic enrichment pattern in proximity to the gold mineralization zone, irrespective of the host rock. Significant presence of Sb up to 130 ppm is detected especially in the segments associated with quartz veining in DDH-11 and DDH-12. However, Mn, Cr and Ba have generally a low concentration in proximity to gold mineralization segments. Elevated values of Cu, Pb, Zn and Fe are often confined to the highly sulfidic mineralization segments, normally characterized by quartz–carbonate veining. The Fe, Co and Mo contents appear to be relatively higher within the zone, just below the ground surface, which is normally characterized by highly weathered or oxidized subsurface.

Gold is associated with a varying amount of silver and tellurium as electrum- and Au-Ag-Te-bearing mineral phases. Pyrite, arsenopyrite, galena and many other sulfide minerals are also important hosts for submicron gold inclusion. Ratios of Co/Mo, Pb/Zn and Bi/Sb for DDH11 display positive trends to the proximity of gold-mineralization zones (Fig. 11). High Bi/Hg ratio was also correlated with proximity to the gold enrichment zone.

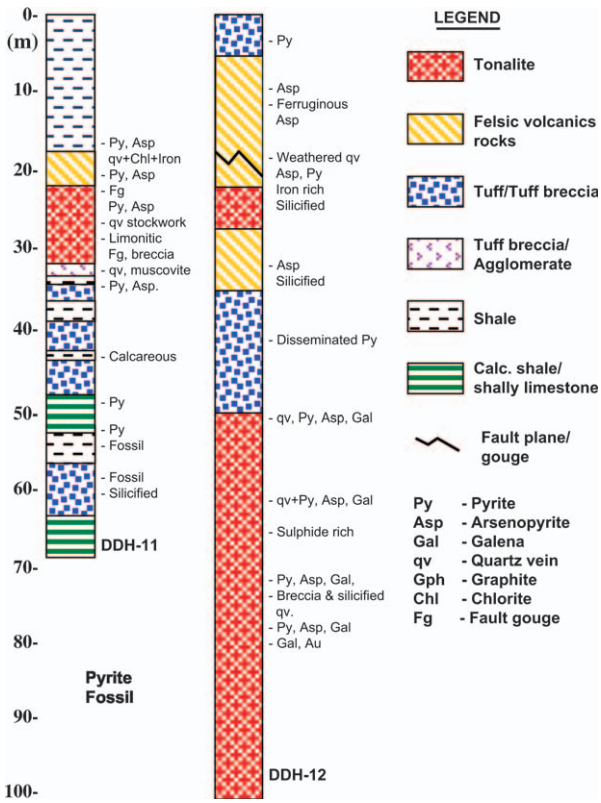

Fig. 9 Geological column of rock types from DDH-11 and DDH-12.

4. Ore mineralogy

The nature and distribution pattern of gold mineralization are studied in detail in an attempt to clarify the texture and morphology of the mineral phases present in the selected ores.

4.1. Quartz-carbonate stringer veinlet

Generally two types of quartz stringer veinlets are recognized, the one associated with sulfide mineralization and the other, clear and barren. Both quartz veinlets are normally clear, milky-white or smoky-white in color. Buff, pinkish white, quartz-feldspar veinlets are also present. Due to strong deformation, the veins are often brecciated and altered with milled grains along the margin. Inclusion of altered wall-rock material is seen infilling the vein fissures. Carbonate is common and forms chiefly quartz–carbonate veins. Mineralization is often found as fissure infilling within quartz–carbonate veins that have been introduced after the deformation. Development of fractures played an important role in the mineralization. Fractures also occur along the intact margin of the quartz–carbonate veins (Fig. 12a, b).

4.2. General features of the ores

Drill core specimens of various rock types and quartz–carbonate veins have been examined. Ores from the Penjom deposit can be broadly divided into four groups, namely vein, dissemination, massive, and fragmental. Sulfide minerals, mainly arsenopyrite and pyrite, are dominant constituents embedded in quartz–carbonate veins (Fig. 12d–f).

The gangue minerals associated with gold mineralization include quartz, feldspars, calcite, ankerite, dolomite, siderite, minrecordite, epidote, manganite, graphite and muscovite (sericite), talc, chlorites, fuchsite, goethite, limonite, fluorite, carbonaceous matters, pyrolusite and kaolinite. Both the veining and massive ores can be subdivided on the basis of their mineral constituents into (i) gold–galena–tetrahedrite–tellurides (especially altaite) ore; (ii) gold–arsenopyrite–pyrite ore; and (iii) pyrite.

Mineralization mainly in quartz–carbonate veins is preferentially confined to the late carbonates. The carbonate consists of clear calcite, siderite, dolomite,

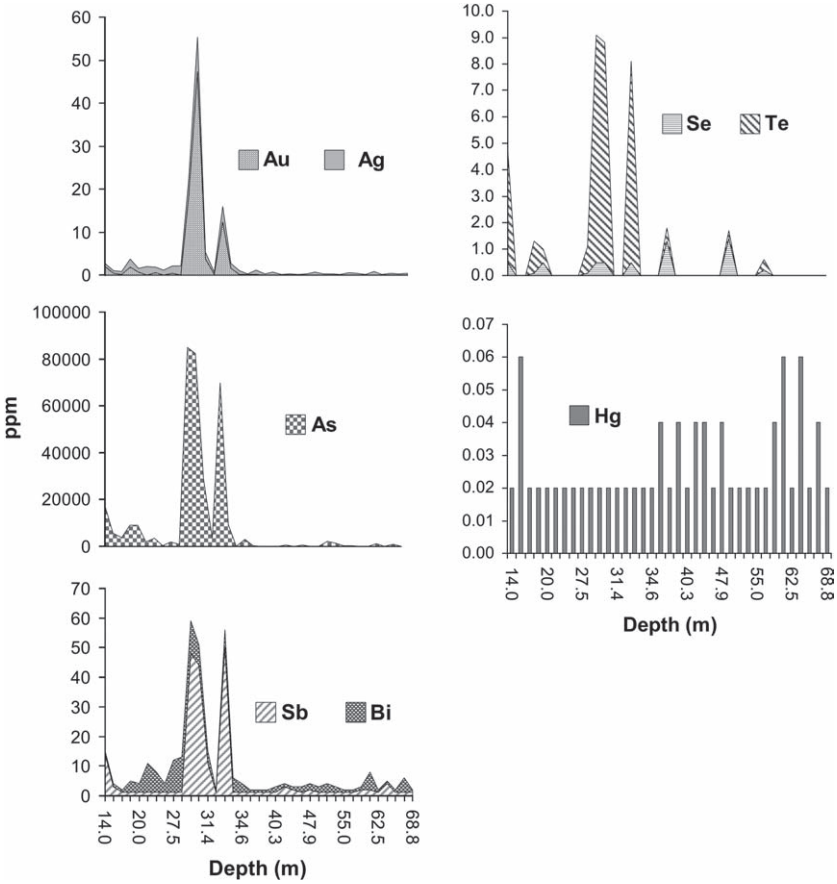

Fig. 10 Multi-elemental distribution patterns against the depth of the Penjom gold mineralization rock formation from DDH-11.

ankerite, minrecordite and murky carbonate. They normally occur along the corroded margin of quartz crystals. The quartz–carbonate system of gold mineralization at Penjom apparently can be distinguished into four different types: (i) quartz–dolomite–ankerite–calcite veining; (ii) quartz–calcite veining; (iii) quartz veining; and (iv) calcite stringer. The gold mineralization is entirely associated with the first two types, and the gold is located only in the clear carbonate.

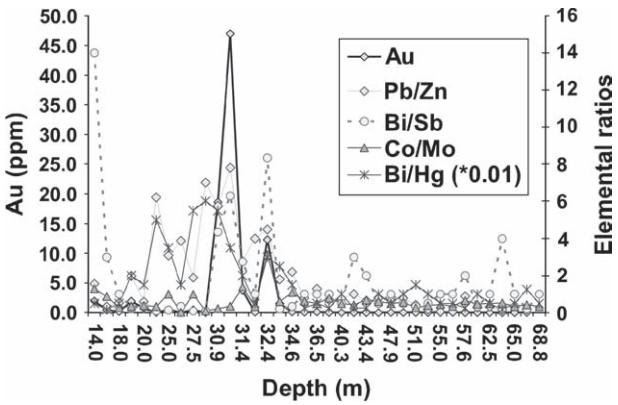

Fig. 11 Distribution of selected elements with regard to geochemistry of DDH-11 associated with gold mineralization pattern.

The sulfide minerals and gold occupy fractures and interstitial spaces within the clear carbonate, locally overprinting them. These mineral phases are often overprinted by murky carbonate. The early quartz veins are mostly barren. A cereous edge is developed between quartz and carbonate phases, where quartz is corroded and replaced by carbonates. Corroded quartz fragments are often enclosed in late carbonates (Fig. 12a). Some gold aggregates are electrum containing >20% silver.

4.3. Pyrite and arsenopyrite

Pyrite is the most widespread sulfide mineral in all types of mineralization, either as isolated idiomorphic crystal, angular to strongly brecciated fragment, colloform aggregates and corroded (rounded off)

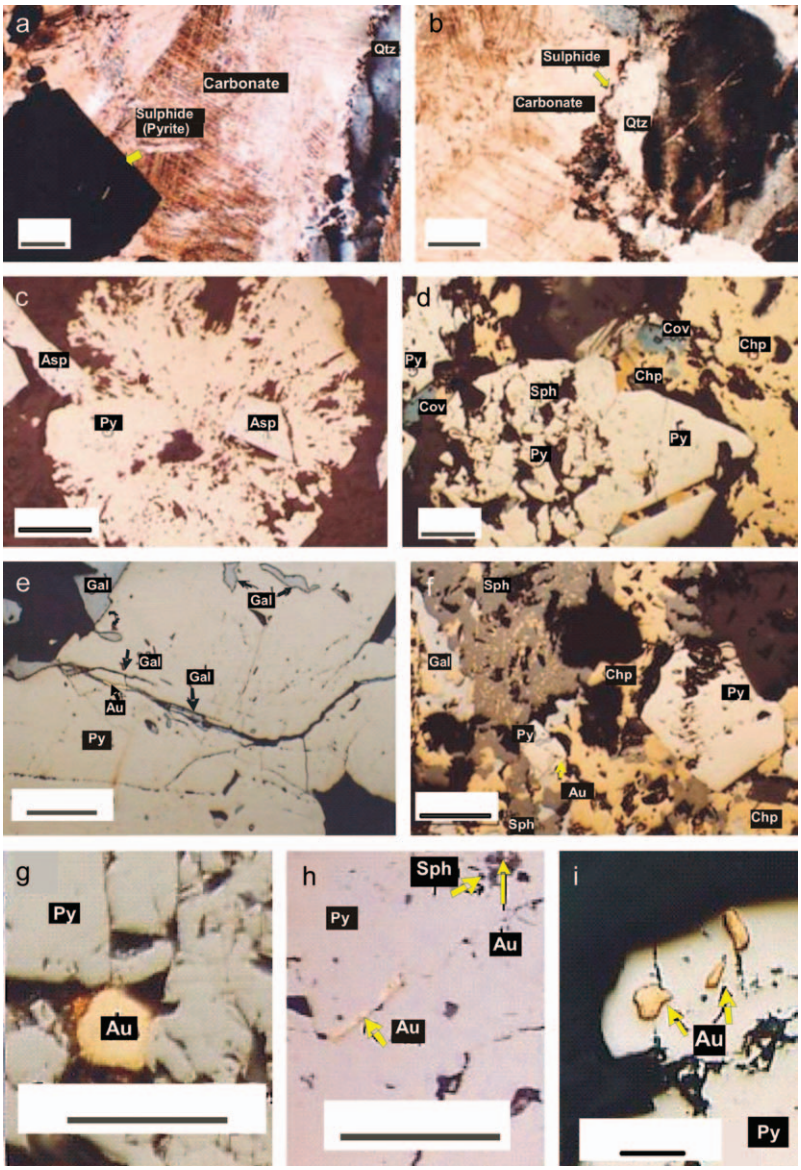

Fig. 12 Photomicrographs of ore minerals in the Penjom deposit. (a, b) brecciated quartz–carbonate vein with sulfide mineralization (pyrite) occupying fissures along the margin sandwiched between carbonate (calcite) and quartz as seen under thin section (DDH12: 86.25 m), (c) individual highly corroded and pitted colloform pyrite (Py) grain enclosing a subhedral arsenopyrite (Asp) crystal. Other arsenopyrite crystals are also visible around the rim of the pyrite. (d) Highly brecciated pyrite (Py) being replaced by chalcopyrite (Chp) with covellite (Cov) along the margin. Minor occurrence of sphalerite (Sph) and galena are also evident. (e) Galena (Gal) and gold (Au) occupying hair-like fractures and pits in pyrite; (f) complex mineralization of sphalerite (Sph), galena (Gal) and chalcopyrite (Chp) in quartz–carbonate vein traversing graphitic shale. Tiny 15 μm gold (Au) is in a fracture in a pyrite (Py) crystal, and (g–i) submicroscopic gold (Au) and sphalerite (Sph) infilling interstices and pits in pyrite. Bars: a, 50 μm; b, 50 μm; c, 100 μm; d, 50 μm; e, 100 μm; f, 100 μm; g, 50 μm; h, 50 μm; i, 100 μm.

aggregates (Fig. 12a, e, f). Pyrite is formed preferentially in carbonate of quartz–carbonate veins. These pyrites often inhabit brittle fractures or interstices within carbonate, including along the margins of veins. The cubic pyrite are common in tonalite and black carbonaceous shale. In veins, pyrite is often seen as corroded and pitted fragments. This pyrite is strongly brecciated locally due to the brittle deformation. Pyrite is also often present, either as isolated grains or clusters that are often characterized by round-off morphology. In particular cases annealed texture of recrystallized pyrite is also evident. Pyrite is partially enclosed by galena and chalcopyrite, and occasionally and marginally replaced and occupied by arsenopyrite (Fig. 13a, c, j). The brittle cracks and pits in pyrite are frequently infilled with galena, arsenopyrite as well as marcasite in places. Certain fissures are also partially occupied by the late sulfide phases such as sphalerite, chalcopyrite and less common, pyrrhotite, covellite and tellurides.

Arsenopyrite seems to be formed later than pyrite but pre-dates the brittle deformation. In many ore specimens, arsenopyrite commonly occurs as fine to coarse discrete grains and aggregates up to 5 mm in

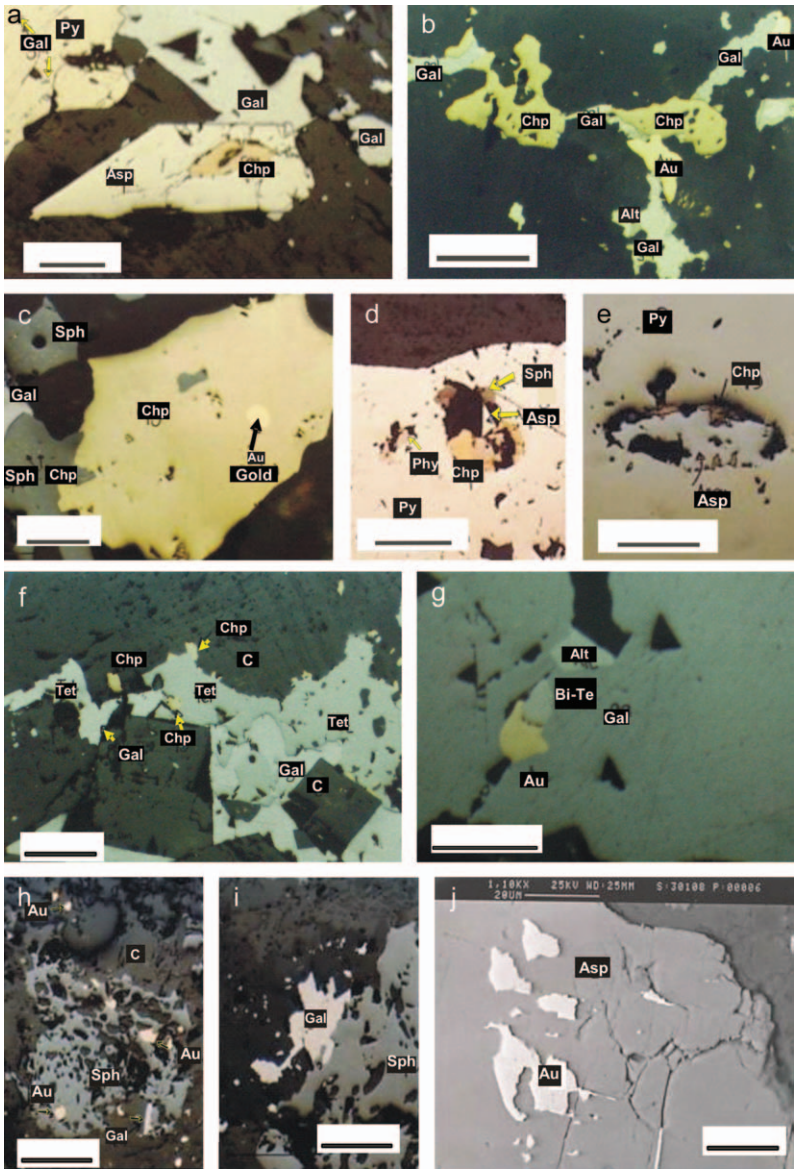

Fig. 13 Photomicrographs of ore minerals in the Penjom deposit. (a) Chalcopyrite (Chp) is seen occupying a pit in subhedral arsenopyrite (Asp). Galena (Gal) is seen occupying tiny pits in pyrite (Py) and replacing both sulfides, (b) carbonate matrix of quartz–carbonate vein shows fractures infilled by chalcopyrite (Chp), while altaite (Alt) and galena (Gal) are intergrown, replacing chalcopyrite (Chp) with the occurrences of tiny electrum, (c) chalcopyrite (Chp) is being replaced by sphalerite (Sph), which in turn is replaced by galena (Gal). An inclusion of submicroscopic gold (15 μm) embedded in chalcopyrite is also visible, (d, e) arsenopyrite (Asp), chalcopyrite (Chp), sphalerite (Sph) and pyrrhotite (Phy) occupying fractures and pits in pyrite, (f) jagged tetrahedrite (Tet), which is being replaced by galena (Gal), and chalcopyrite (Chp) occupied the interstices in the calcite (C) of quartz–carbonate vein, (g) electrum (Au) is seen associated with light brownish grey bismuth–telluride BiTe(Pb)-tetradymite and altaite(Alt) enclosed in massive galena (Gal), (h) sphalerite intergrown with galena and gold blebs locally within the quartz–carbonate vein (C-calcite), (i) irregular shaped sphalerite (Sph) intergrown with (Gal), and (j) back-scattered electron image shows gold (Au) infilling the interstitial spaces and fractures of arsenopyrite (Asp). Bars: a, 100 μm; b, 100 μm; c, 100 μm; d, 100 μm; e, 100 μm; f, 100 μm; g, 100 μm; h, 100 μm; i, 100 μm; j, 20 μm.

size. Grains of variable sizes are disseminated within the host rocks and preferentially in carbonate of quartz–carbonate vein. Thin bands of fine-grained arsenopyrite and larger individual subhedral crystals are found in graphite in carbonaceous shale. They are locally developed along the contact or margin between the quartz–carbonate vein and the wall rock. Most of the coarse arsenopyrite grains are often highly fractured, brecciated, milled and pitted with irregular boundaries as well as oxidized grains. This has resulted in the formation of caries texture in some arsenopyrite crystals. Arsenopyrite grains developed in the carbonaceous schist often with internal ghost structure inherited from the schist.

4.4. Native gold and electrum

Gold occurrences, normally as electrum, are noticeable in various type of ore, often in minor amounts as fine disseminated particles (up to 200 μm) infilling fractures, pits and interstices throughout quartz–carbonate and sulfide minerals. The aggregate preferentially occurs as infillings in interstitial spaces and grain boundaries of carbonates in quartz–carbonate vein, where

fine-grained free gold particles often occur along the mutual contact between calcite and quartz. It is also found in graphitic streaks and fragments of these veins, which are closely associated with carbonaceous rocks.

Submicroscopic gold is also found in fractures and pits of fractured pyrite and arsenopyrite, as well as clinging to the arsenopyrite perimeter. Fine-grained gold is also found in interstitial spaces in sphalerite, chalcopyrite, pyrite, hessite, galena and molybdenite and as inclusions in these sulfides and tellurides, and intergrown with tellurides and galena. Gold was observed adhering or adjacent to the surface of fractured and corroded arsenopyrite aggregates. Gold is also found as infilling pits in pyrite, sphalerite and chalcopyrite. Various gold occurrences are shown in Figures 12(e–i) and 13(b, c, j). Electrum occurs in substantial amount, and often closely associated with gold and tellurides-bearing minerals. EDX analysis has confirmed that most of the examined specimen's Ag content of electrum is >20% silver, frequently in the range of 20–30% (Kamar Shah, 1995). Electrum often occurs as fine aggregates intergrown with galena, altaite or infilling fractures of arsenopyrite and pyrite or interstices of carbonate and other sulfides locally.

4.5. Galena

Galena is the third abundant sulfide and is formed after sphalerite and chalcopyrite. It occurs as fine to coarse aggregates, infilling interstices and microfractures within the quartz–carbonate veins system. Galena often replaces tetrahedrite, chalcopyrite and sphalerite, apart from infilling fractures and pits of earlier brecciated pyrite and arsenopyrite within the mineralization zone as well as intergrown aggregate with telluride as shown in Figure 13(a, b, f, g). Galena is closely associated with gold mineralization, where microscopic gold particles frequently infill pits and interstices of galena, often overprinting it.

4.6. Chalcopyrite

The presence of chalcopyrite is normally in association with other sulfides in minor amounts and almost entirely in the form of chalcopyrite disease or blebs in sphalerite (Barton & Bethke, 1987) as shown in Figures 12(f) and 13(c, h, i). Chalcopyrite formed also after brittle deformation as fine to coarse, disseminated aggregates either within host rocks or infilling interstices of carbonate in quartz–carbonate veins. This mineral is also found occupying pits or replacing the corroded pyrite, arsenopyrite, tetrahedrite and sphalerite locally (Figs 12f, 13d–f).

4.7. Sphalerite

Sphalerite is formed after brittle deformation, but earlier than chalcopyrite and galena. It often occurs as fine discrete grains and aggregate (up to 4 mm) disseminated in the host rock, as fracture-fillings in pyrite and arsenopyrite and within interstices of carbonates in quartz–carbonate vein. It is also frequently intergrown with chalcopyrite, tetrahedrite and galena, and often contains chalcopyrite disease and blebs (Fig. 12d, f). Galena, telluride and gold are also found as fine aggregate occupying interstitial spaces of sphalerite (Fig. 13h, i).

4.8. Tetrahedrite

Tetrahedrite is a post-deformation mineral that is normally found in minor amounts as fine to coarse aggregate (up to 1 mm) infilling interstices of quartz–carbonate veins. It is locally, along the margin, replaced by chalcopyrite and galena (Fig. 13f).

4.9. Tellurides

Telluride occurrences as verified using EDX microprobe are closely associated with other sulfides, and frequently intergrown with galena and gold, infilling interstices of arsenopyrite, sphalerite, chalcopyrites, galena, tetrahedrite and carbonate in quartz–carbonate veins (Fig. 13b, g). Among common species identified, usually in minor amounts of aggregate up to 300 μm, are hessite (Ag_2Te), altaite ($PbTe_2$), petzite (Ag_3AuTe_2), sylvanite ($AuAgTe_4$) and tetradymite (Bi_2TeS) as shown in Figure 13g; and possibly calaverite ($AuTe_2$) and wehrlite ($BiTe_2$).

4.10. Covellite and digenite

Covellite and digenite occur in minor amounts as alteration products of chalcopyrite. They are clearly of secondary origin due to their occurrence as replacement or chemical reaction rims along the margin and fractures of chalcopyrite (Fig. 12d).

4.11. Graphite

Numerous graphite is present in country rock affiliated with graphitic schist as low-rank coal-type in nature. Inclusions of graphitic materials are also noticed

within many quartz–carbonate veins, hosted within carbonaceous shale in places.

5. Ore genesis

The paragenetic sequence (Fig. 14) of mineralization starts right after an early phase of ductile deformation that gives rise to the development of pervasive foliation as in carbonaceous shale, but less developed in tuff. However, ductile deformation occurs locally within silicified rhyolites that is invaded by quartz–carbonate veins. This activity was followed by the subsequent influx of hydrothermal activities that introduced silica-rich fluid into the dilatant zones.

Subsequent brittle deformation led to fracturing and brecciation with dilatant zone infilled by quartz veins. The fluid inclusion study conducted by J. R. Herrington (unpubl. data, 1992) suggests the presence of two broad hydrothermal fluids of primarily low salinity, H_2O-CO_2-salts-bearing fluid with homogenization temperatures of 270°–280°C and secondary H_2O-salts-bearing fluid with homogenization mean around 140°C. It appears that the higher temperature (>270°C) carbonic fluid, which was probably gold-bearing, was introduced into the vein system that characterizes many mesothermal vein deposits.

The earliest mineralization is the development of coarse-grained pyrite and arsenopyrite in graphitic schist unit that has pre-dated the brittle deformation, because these two minerals are severely fractured and brecciated. Subsequently sphalerite and tetrahedrite, together with chalcopyrite, were deposited. These minerals were also affected locally by brittle deformation, but less intensely than arsenopyrite. A subsequent phase was characterized by the influx of carbonate-rich fluid carrying gold. The precipitation of quartz–calcite together with electrum, molybdenum, tetrahedrite and other tellurides and bismuth, infilled the caries structure.

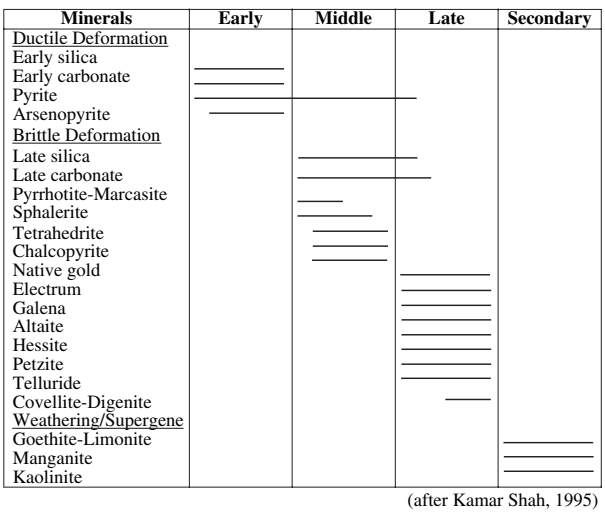

Fig. 14 General paragenesis sequence of gold ore mineralization from Penjom gold deposit.

Microscopic observations suggest that the formation of sphalerite, chalcopyrite and tetrahedrite continued during the influx of gold-bearing solutions into the system. However, most of the gold deposition took place after the precipitation of these sulfides. Galena appeared towards the end of gold mineralization, whereas tellurides and bismuth accompanied gold mineralization contemporaneously.

Primary gold mineralization in the Penjom area occurred in a complex structural setting associated with volcanics with a sequence of marine sediments intruded by minor tonalite. Boyle (1979), Kwong and Crocket (1978), Cherry (1983) and Schroeter and Cameron (1996) stressed that all gold is bound to acid granitic magmas, and in particular the metal is associated with SiO_2. Typical gold carriers are the granodiorites and granites and are situated in close proximity to clastic or chemical sediment. At Penjom the source of gold is more likely to be magmatic because of the widespread occurrences of intrusive igneous rocks of I-type granitic character in the surrounding neighbourhood. In contrast, tuffaceous sediments and graphitic shale of the Padang Tengku Formation also constitute favorable crustal sources for gold.

The genesis of the deposits was controversial but some workers favor a metamorphogenic deformational origin, rather than the low-sulfidation epithermal one favored by Corbett (2002). Because the formation of the Penjom deposits is associated with widespread occurrence of mantle plume-type magmatism of Central Belt plutons (Hutchison, 1971, 1977; Mustaffa Kamal & Azman, 2003), a magmatic influence in their genesis was one of the accepted explanations.

6. Conclusions

The Penjom gold mineralization is regarded as high-grade quartz–carbonate–gold type related to a phyllic-propylitic alteration of tonalite complex that intrudes weakly metamorphosed sedimentary strata. At Penjom, ore systems display permeability controlled or governed by lithology, structure and breccias and changes in wall-rock alteration (quartz, carbonate, sericite, chlorite, fuchsite and clay). Widespread

occurrences of pyrite, sphalerite, galena, chalcopyrite, arsenopyrite, molybdenite, tetrahedrite, and tellurides, gangue minerals including quartz, carbonates (calcite, ankerite, dolomite and siderite) and graphite basically coincide with formation of polymetallic gold–silver ore and are in transition to higher crustal level of carbonate–base metal class. Penjom, and almost all of the other *in situ* gold deposits in Peninsula Malaysia, are classified as epizonal orogenic lode (low mesothermal) gold deposit after Groves *et al.* (1998) rather than magmatic arc-hosted epithermal systems (J. R. Herrington, unpubl. data, 1992; Kamar Shah, 1995; Flindell, 2003; Wan Fuad & Heru Sigit, 2003).

Acknowledgments

This work was part of the Masters thesis program of the senior author undertaken with close cooperation of Specific Resources Sdn. Bhd., Avocet Venture, which provided the necessary access, logistics and financial assistance that made this research feasible. This research was the outcome of the early stage of exploration work undertaken to study and evaluate the nature of geology and gold mineralization of the Penjom gold prospect under awarded concession Block 7, Pahang in early 1991–1994. The authors acknowledge the contribution and guidance given by David Crips, Mian Khalid Habib, Eric K. H. Goh and Paul Ponar Sinjeng towards the completion of the research as well as to Universiti Sains Malaysia. Thanks are also due to Akira Imai, Kyushu University, Japan and I Wayan Warmada, Gadjah Mada University, Indonesia for their constructive comments on the paper.

References

Ahmad, J. (1979) The petrology of the Gunung Benom igneous complex. Geological Survey Malaysia, Special Paper, 2, 141p.

Alexander, J. B. (1949) Progress report on geological work in southwest Pahang and in part of northwest Selangor. Malaya Geological Survey, Annal report. Government Press, Kuala Lumpur, 19–24.

Azman, A. G., Ramesh, V., Yong, B. T. and Khoo, T. T. (2006) Geochemistry and petrology of syenite, monzonite and gabbro from the Central Belt of Peninsular Malaysia. Geol. Soc. Malays. Bull., 49, 25–30.

Barton, P. B. Jr. and Bethke, P. M. (1987) Chalcopyrite disease in sphalerite: Pathology and epidemiology. Am. Mineral., 72, 451–467.

Becher, H. M. (1983) The gold–quartz deposits in Pahang (Malay Peninsula). Quaternary J. Geol. Soc., Lond., 49, 84–88.

Bignell, J. D. and Snelling, J. B. (1977) The geochronology of Malayan granite. Overseas Geol. Miner. Res. Inst. Geol. Sci. Lond., 47, 358–359.

Boyle, R. W. (1979) The geochemistry of gold and its deposits. Can. Geol. Surv. Bull., 280, 584p.

Campi, M. J., Shi, J. R. and Leman, M. S. (2002) The *Leptodus* Shales of central Peninsular Malaysia: Distribution, age and palaeobiogeographical affinities. J. Asian Earth Sci., 20, 703–717.

Cherry, M. E. (1983) The association of gold and felsic intrusion: Examples from Abitibi Belt. The geology of gold in Ontario. Ontario Geol. Surv. Miscell. Paper, 110, 48–55.

Chu, L. H. and Singh, D. S. (1984) The nature and potential of gold mineralization in Kelantan, Peninsular Malaysia. In GEOSEA V Proceedings. Geol. Soc. Malays. Bull., 19, 431–440.

Cocks, L. R. M., Fortey, R. A. and Lee, C. P. (2005) A review of lower and middle palaeozoic biostratigraphy in west peninsular Malaysia and southern Thailand in its context within the Sibumasu Terrane. J. Asian Earth Sci., 24, 703–717.

Corbett, G. (2002) Epithermal gold for explorationist. e-AIG Journal, April, 1–26.

Fillis, P. (2000) Penjom resource model. Unpublished internal report for Specific Resources Sdn. Bhd. Kuala Lipis, Specific Resources, Pahang, Malaysia, 4p.

Flindell, P. (2003) Avocet mining: Exploration and development across central and Southeast Asia. Australia Institute of Geoscientists (AIG), Mineral Exploration Discussion Group (SMEDG), 10 October, Sydney. Australian Institute of Geoscientists, Perth, 8p.

Gobbett, D. J. and Hutchison, C. S. (1973) Geology of the Malay Peninsular, West Malaysia and Singapore. Wiley Interscience, New York, 438p.

Groves, D. I., Goldfarb, R. J., Gebre-Mariam, M., Hageman, S. G. and Robert, F. (1998) Orogenic gold deposits: A proposed classification in the context of their crustal distribution and relationship to other gold deposit. Ore Geol. Rev., 13, 7–27.

Hutchison, C. S. (1971) The Benta magmatite complex: Petrology of two important localities. Geol. Soc. Malays. Bull., 4, 49–70.

Hutchison, C. S. (1977) Granite emplacement and their tectonic subdivision of Malay Peninsula. Geol. Soc. Malays. Bull., 9, 187–207.

Kamar Shah, A. (1995) Geology and mineralogy of the Penjom gold mineralization prospect. Unpublished MSc Thesis, Universiti Sains Malaysia, Penang, Malaysia.

Kamar Shah, A. and Khairun Azizi, M. A. (1995) An overview of the mineralization and mineralogical characteristic of the goldfields from Central Belt of Peninsular Malaysia. *In* Proceeding of the International Conference on Geology, Geotechnology and Mineral Resources of Indochina, Khon Khean, Thailand. Khon Khean University, Khon Khean, 188–199.

Khoo, T. T. and Tan, B. K. (1983) Geological evolution of Peninsular Malaysia. In Proceeding of the Workshop on Stratigraphic Correlation of Thailand and Malaysia, 1, 253–290.

Kobayashi, T. and Toriyama, R. (1970) Geology and palaeontology of South East Asia. University of Tokyo Press, Japan, 1–25.

Kwong, Y. T. and Crocket, J. H. (1978) Background and anomalous gold in rocks of an Archean greenstone assemblage, Kagaki Lake Area, N.W. Ontario. Econ. Geol., 73, 50–63.

Lee, A. K., Gonzales, R. A., Tyebally, F. H., Chand, F. and Troup, A. (1982) Regional geochemistry of North Pahang. Geol. Surv. Malays. Geochem. Rep., 2, 86p.

Lee, A. K., Khong, Y. and Hock, O. W. (1986) Gold mineralisation and prospects in North Pahang. Geol. Surv. Malays. Geochem. Rep., 4, 50p.

Leman, M. S. (1994) The significance of upper Permian brachiopods from Merapoh area, northwest Pahang. Geol. Soc. Malays. Bull., 35, 113–121.

Metcalfe, I. (1988) Origin and assembly of Southeast Asian continental terranes, Gondwana and Tethys. *In* Audley-Charles, M. G. and Hallam, A. (eds.) Geological Society of London Special Publication, 37, 101–118.

Metcalfe, I. (1992) Lower Triassic (Smithian) Conodon from northwest Pahang, Peninsular Malaysia. J. Micropaleontol., 11, 13–19.

Metcalfe, I. (2000) The Bentong-Raub Suture Zone. J. Asian Earth Sci., 18, 691–712.

Metcalfe, I. (2002) Permian tectonic framework and palaeogeography of SE Asia. J. Asian Earth Sci., 20, 551–566.

Mitchell, A. H. G. (1977) Tectonic setting for emplacement of southeast Asian tin granite. Geol. Soc. Malays. Bull., 9, 123–140.

Mohd Rozi, U. and Sheikh Almashoor, S. (2000) Jujukan Usia Batuan di Dalam Kompleks Benta, Pahang Berdasarkan Cirian Lapangan dan Penentuan Usia Batuan Secara K/Ar Keseluruhan Batuan. *In* Proceedings of the Annual Geological Conference, Geological Society of Malaysia, Penang. Geological Society of Malaysia, Penang, 87–95.

Mustaffa Kamal, S. and Azman, A. G. (2003) 'Mantle Plume' type magmatism in the Central Belt Peninsular Malaysia and its tectonic implications. Geol. Soc. Malays. Bull., 46, 365–371.

Nancy, T. (1972) Carboniferous fossils from "Raub Group" near Chuak Village, Western Pahang, West Malaysia. Geol. Soc. Malays. Bull., 34, 5–9.

Nuraiteng, T. A. (1993) The occurrence of upper Permian foraminifera in NW Pahang. Proceeding of the 24th Annual Geological Conference, Technical Paper, 3, 25–33.

Pereira, J. J. (1993) Geology, mining and tailing characteristic of the Selinsing Gold Mine, Pahang. Warta Geologi, Newslett. Geol. Soc. Malays., 19, 35–41.

Pereira, J. J., Yeap, E. B. and Ng, T. F. (1993) Application of soil geochemistry to the detection of Sb-Au mineralization in the Buffalo Reef Area. Geol. Soc. Malays. Bull., 33, 1–10.

Proctor, W. D. (1972) Geology and mineral resources Benta Area, Pahang. Geol. Surv. Malays., Map Bull., 4, 25p.

Richardson, J. A. (1939) The geology and mineral resources of the neighbourhood of Raub, Pahang with an account of the geology of the Raub Australian Gold Mine. Geological Survey Malaysia, Kuala Lumpur, 3, 162p.

Richardson, J. A. (1950) The geology and mineral resources of the neighborhood of Cegar Perah and Merapoh, Pahang. Geol. Surv. Malays. Mem., 4, 162p.

Santokh Singh, D. (1977) Gold mineralization in Peninsular Malaysia, National seminar on the mining industry. Ministry of Primary Industries, Malaysia, 8p.

Schroeter, T. G. and Cameron, R. (1996) Alkalic Intrusion-associated Au-Ag. *In* Lefebure, D. V. and Hoy, T. (eds.) Selected British Columbia Mineral Deposits Profiles, Vol. 2: Metallic Deposits. Open File 1996-13. British Columbia Ministry of Employment and Investment, Victoria, Canada, 49–51.

Schwartz, M. O., Rajah, S. S., Askury, A. K., Putthapiban, P. and Djaswadi, S. (1995) The Southeast Asian Tin Belt. Earth Sci. Rev., 38, 95–293.

Scrivenor, J. B. (1911) The geology and mining industries of Ulu Pahang. Government Press, Malaya, 216p.

Scrivenor, J. B. (1928) The geology of the Malaysia Ore Deposit. MacMillan & Co., London, 216p.

Scrivenor, J. B. (1931) The geology of Malaya. MacMillan, London, 250p.

Sinjeng, P. P. (1993) Mineralogy of gold bearing rocks from the Mengapur Ore deposit. Proceeding of the 24th Annual Geological Conference, Technical Paper, Vol. 3. Geological Survey of Malaysia, Kuala Lumpur, 25–33.

Sonny, L. T. C., Sharafuddin, M., Sulaiman, M., Teh, G. H. and Abdul Aziz, J. H. (2001) Geology, structure, mineralization and geochemistry of the Penjom gold deposit, Penjom, Pahang. Geol. Soc. Malays. Bull., 44, 61–63.

Spiller, F. C. P. and Metcalfe, I. (1995) Late palaeozoic radiolarians from the Bentong-Raub suture zone and Semanggol Formation, Peninsular Malaysia: Initial finding. J. Southeast Asian Earth Sci., 11, 217–224.

Tan, B. K. (1984) The tectonic framework and evaluation of the Central Belt and its margin, Peninsular Malaysia. Geol. Soc. Malays. Bull., 17, 307–322.

Tan, B. K. (1996) "Suture Zone" in peninsular Malaysia and Thailand: Implications for paleotectonic reconstruction of Southeast Asia. J. Southeast Asian Earth Sci., 13, 243–249.

Tjia, H. D. (1987) Olistostrome in the Bentong area, Pahang. Warta Geologi, 13, 105–111.

Tjia, H. D. (1989) The Bentong suture. *In* Situmorang, B. (ed.) Proceedings of the 6th Regional Conference on Mineral and Hydrocarbon Resources SE Asia. Indonesian Association of Geologists, Jakarta, 73–85.

Tjia, H. D. and Zaitun, H. (1985) Regional structures of Peninsular Malaysia. Sains Malaysiana, 14, 95–107.

Wan Fuad, W. H. and Heru Sigit, P. (2001) Perubahan batuan dinding berkaitan dengan permineralan emas di Penjom Gold Mine, Pahang, Malaysia. *In* Proceedings, Geological Society of Malaysia, Annual Geological Conference, Pangkor, Malaysia. Geological Society of Malaysia, Kuala Lumpur, 13–17.

Wan Fuad, W. H. and Heru Sigit, P. (2003) Analisis bendalir terkepung pada terlerang kuarza yang mengandungi emas di kawasan lombong Penjom, Kuala Lipis, Pahang dan Lubok Mandi. Geol. Soc. Malays. Bull., 46, 359–363 (in Malaysian).

Yeap, E. B. (1993) Tin and gold mineralization in Peninsular Malaysia and their relationships to the tectonic development. J. Southeast Asian Earth Sci., 8, 329–348.

Yong, B. T., Azman, A. G., Khoo, T. T. and Shafari, M. (2004) Benom complex: evidence of magmatic origin. Geol. Soc. Malays. Bull., 47, 55–60.